JOURNAL OF MATERIALS SCIENCE 20 (1985) 2399–2407

The microstructure and mechanical properties of yttria-stabilized zirconia prepared by arc-melting

TAKETO SAKUMA, YU-ICHI YOSHIZAWA, HAJIME SUTO
Department of Materials Science, Faculty of Engineering, Tohoku University, Sendai, Japan

The microstructure of ZrO_2–Y_2O_3 alloys prepared by arc-melting was examined mainly by electron microscopy. It was found that the microstructure changed markedly with yttria content between 0 and 8·7 mol %. Pure zirconia was a single monoclinic phase, while ZrO_2–8·7 mol % Y_2O_3 alloy was single cubic phase as expected from ZrO_2–Y_2O_3 phase diagram. Tetragonal phase was found in alloys with 1 to 6 mol % Y_2O_3 together with monoclinic or cubic phase. The tetragonal phase found in present alloys normally had a lenticular shape with a length 1 to 5 μm and a width 0.1 to 0.3 μm, which is much larger than that formed by annealing. The phase with a herring-bone appearance was found in alloys with Y_2O_3 between 2 and 3 mol %, which was recognized to be a metastable rhombohedral phase. The structure of the present alloys is likely to be formed by martensitic or bainitic transformation during fairly rapid cooling from the melt temperature. The change in hardness and toughness with yttria content of the alloys is discussed on the basis of microstructural observations.

1. Introduction

Partially-stabilized zirconia (PSZ) is toughened by the dispersion of metastable tetragonal particles in a cubic matrix [1–5]. It has generally been accepted that the toughness increase in PSZ is principally attributed to energy absorption near the advancing crack tip due to the tetragonal-to-monoclinic phase transformation of the particles [6–11]. The stability of the tetragonal phase (t-phase), therefore, plays an important role in the strength and toughness of PSZ. It is well-known that PSZ is prepared by adding a suitable amount of fluorite-stabilizing oxides such as CaO, MgO and Y_2O_3 to ZrO_2. An analysis of the X-ray intensity profile has revealed that the amount of t-phase is strongly influenced by the composition of PSZ as well as the sintering temperature and soaking time [12]. It has also been clarified that the mechanical property of PSZ is markedly affected by microstructural change during ageing in the cubic/tetragonal two-phase region [5, 13]. The dispersion of t-phase in cubic matrix is another factor to control the mechanical property of PSZ. However, the relationship between microstructure and mechanical property has not fully been understood yet. This is partly related to the fabrication process of PSZ, which is ordinarily prepared from zirconia powders and yttria or other fluorite-stabilizing oxide powders by sintering or hot pressing. The PSZ thus obtained often has a local compositional fluctuation which causes the nonuniformity of microstructure. The mechanical property of PSZ is affected not only by the nonuniformity of structure but also by many other factors such as grain size, porosity and type of sintering aids. It is, therefore, not straightforward to understand the relationship between microstructure and mechanical properties of PSZ. In the present study, various ZrO_2–Y_2O_3 alloys with uniform composition were prepared by arc-melting and the change in microstructure with yttria content was examined in detail. The change in hardness and toughness of zirconia with yttria content was discussed from a microstructural view-point.

0022–2461/85 $03.00 + .12

2. Experimental procedure

Zirconia and yttria powders with 99.9% purity produced by the Rare Metallic Co. Ltd. were used for preparing ZrO_2–Y_2O_3 alloys. Oxide powders mixed in a ball mill were pressed into bars and then sintered at 1673 K. The sintered bodies were arc-melted in an argon atmosphere. Arc-melted samples were cooled on a water-cooled copper hearth. Cooling rate was measured by optical pyrometer as $\sim 700\,K\,sec^{-1}$ between melting temperature and 2300 K, and $\sim 100\,K\,sec^{-1}$ between 2300 and 1300 K. The samples were button-shaped with a mass of about 1 g and had columnar grains with average diameter 0.5 mm. They were black in colour due to oxygen deficiency, but restored the usual colour by annealing at 1473 K for several hours in air as reported previously [14]. The oxygen deficiency was estimated to be about 1 at% from weight gain of the samples after the annealing. The composition of the alloys used is listed in Table I. Hereafter, alloy number shown in Table I is used to indicate each alloy. EPMA analysis has revealed that the local compositional change in arc-melted samples is less than 0.5 mol%. Hardness measurements and metallographic examinations were carried out at the as-cast state. X-ray diffraction studies were made by crushed powders of an as-cast button. The specimens for electron microscopy were initially cut from the button-shaped samples and then polished to a disc with a thickness 0.3 mm. Thin foils were prepared from the disc by ion-beam thinning and examined by JEM 200B electron microscope operated at 200 kV. Microanalysis was carried out by JEM 200CX electron microscope with energy dispersive X-ray spectrometer.

TABLE I Composition of alloys used. Yttria content was estimated by EPMA analysis

Alloy number	Yttria content (mol% Y_2O_3)
0	0
1	1.0
2	2.1
3	2.9
4	4.0
5	5.0
6	6.3
8	8.7

3. Results

3.1. Hardness and toughness

Microhardness is shown as a function of yttria content of the alloys in Fig. 1. The hardness rapidly increases with an addition of Y_2O_3 up to about 3 mol%, while further addition of Y_2O_3 results in a gradual decrease in hardness. The hardness of alloy 3 is more than twice as large as that for pure zirconia.

The alloys were usually cracked at the edge of indentation when the hardness measurements were made under a fairly large applied load. Fig. 2 shows Vickers indentations obtained under 500 g load in three alloys. Many fine cracks were intro-

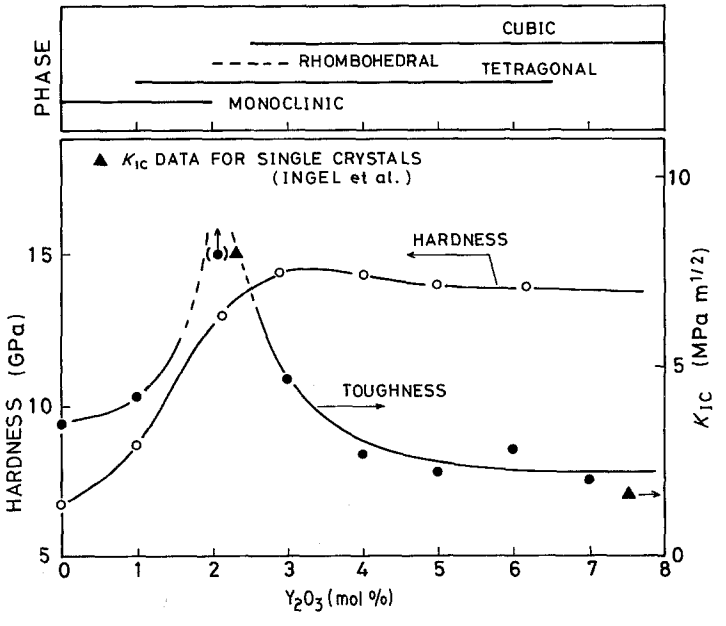

Figure 1 A plot of microhardness and fracture toughness of ZrO_2–Y_2O_3 alloys as a function of yttria content. Open circles and filled circles show the data of microhardness and fracture toughness, respectively. Filled triangles are the data obtained in yttria-stabilized zirconia single crystals [21]. The room-temperature phases in alloys are also shown.

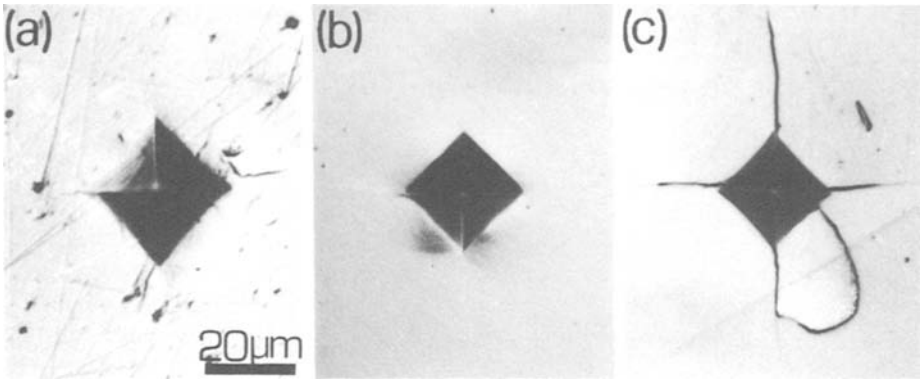

Figure 2 Microhardness indentations in (a) alloy 1, (b) alloy 3 and (c) alloy 5. Cracks are introduced in (a) and (c), but not in (b).

duced around the indentation in alloys 0 and 1 as shown in Fig. 2a, but sharp cracks were developed in alloys with more than 4 mol % Y_2O_3 as shown in Fig. 2c. No cracks were clearly seen in alloys 2 and 3 (Fig. 2b), which are superior in toughness to the other alloys. Observable cracks were usually formed in alloy 3 under 5 kg load, but alloy 2 was seldom cracked even under this load.

The fracture toughness was tentatively estimated by indentation method from the following equations [15]

$$\left(\frac{3K_{IC}}{Ha^{1/2}}\right)\left(\frac{H}{3E}\right)^{2/5} = 0.129\left(\frac{c}{a}\right)^{-3/2} \qquad 2.5 \leqslant \frac{c}{a} \quad (1)$$

for median cracks, and

$$\left(\frac{3K_{IC}}{Ha^{1/2}}\right)\left(\frac{H}{3E}\right)^{2/5} = 0.035\left(\frac{l}{a}\right)^{-1/2}$$

$$0.25 \leqslant \frac{l}{a} \leqslant 2.5 \quad (2)$$

for Palmqvist cracks, where K_{IC} is the Mode I critical stress intensity factor, H is the hardness, E is the Young's modulus, a is the half-diagonal of Vickers indent, c is the radius of surface crack and l is the parameter for crack length which is related to c by

$$\frac{l}{a} = \frac{c}{a} - 1 \quad (3)$$

The data of K_{IC} estimated from Equations 1 and 2 is shown in Fig. 1. The value of K_{IC} of alloy 2 was estimated from the crack which was rarely seen around indents. As cracks were not usually formed in alloy 2, the real value of K_{IC} is expected to be higher than that shown in Fig. 1. It should be noted that the indentation method is not suitable for evaluating K_{IC} of materials with a fracture toughness more than about 10. Despite the fact that the reliability of the indentation method is still in controversy [16–20], the present data agree fairly well with that obtained by the double-cantilever beam technique in ZrO_2–Y_2O_3 single crystals [21]. Fig. 1 shows that the toughness changes markedly with composition of the alloys and has a sharp peak at about 2 mol % Y_2O_3. Although the present alloys were not prepared by a conventional technique, the peak in toughness appears in the alloy with almost the same composition as that for the commercial PSZ.

3.2. X-ray diffraction studies

Crushed powders were examined by X-ray diffractometer at room temperature for identifying the phases in each alloy. Pure zirconia was composed of monoclinic phase (m-phase) at room temperature, as commonly found in previous works [22]. An addition of yttria results in a decreased amount of m-phase and appearance of tetragonal phase (t-phase). It has been shown that the volume fraction of m-phase, $\bar{V}_m$, can be estimated from the following equation [5],

$$\bar{V}_m = \frac{1.603[I(1\,1\,\bar{1})_m]}{1.603[I(1\,1\,\bar{1})_m] + I(1\,1\,1)_c} \quad (4)$$

$I(1\,1\,\bar{1})_m$ and $I(1\,1\,1)_c$ in Equation 4 are the integrated intensities of $(1\,1\,\bar{1})_m$ and $(1\,1\,1)_c$ peaks, where subscript m or c shows m-phase or cubic phase (c-phase), respectively. The value of $\bar{V}_m$ estimated from Equation 4 is shown in Fig. 3 as a function of yttria content of alloys. The relationship between $\bar{V}_m$ and yttria content in the present

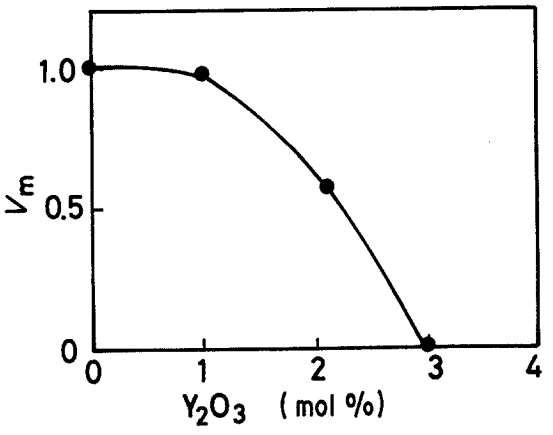

Figure 3 Volume fraction of monoclinic phase determined by X-ray diffraction as a function of yttria content.

alloys has a similar tendency with that obtained in sintered PSZ [12]. The amount of m-phase drastically decreases with increasing yttria content and the m-phase has completely disappeared in the alloys with more than 3 mol% Y_2O_3. The marked increase in hardness with a yttria addition up to 3 mol% (Fig. 1) corresponds to a rapid decrease in $\bar{V}_m$ with yttria content.

The volume fraction of t- and c-phases in various alloys was not quantitatively estimated, because most of the peaks from t- and c-phases were overlapped. However, X-ray intensity profiles around the $(4\,0\,0)_c$ peak and electron microscopy have qualitatively shown that the amount of t-phase decreases with increasing yttria content.

3.3. Change in microstructure with Y_2O_3 content

As confirmed by X-ray diffraction studies, pure zirconia consists of single m-phase at room temperature. The m-phase is ordinarily twinned as shown in Fig. 4, which is easily distinguished from c- or t-phase by electron diffraction. The twin plane of the m-phase is either $\{1\,0\,0\}_m$ or $\{1\,1\,0\}_m$ plane as reported previously [23, 24].

The volume fraction of m-phase in the thin foils prepared from the as-cast buttons of alloys 2 and 3 was smaller than that estimated by X-ray diffraction. For example, m-phase was not commonly seen in alloy 2 by electron microscopy. The result seems to show that the t-phase in the alloys was partly transformed to m-phase during crushing the as-cast button for X-ray diffraction experiment. The m-phase was not found in alloys with more than 3 mol% Y_2O_3. The principal phases in alloys with 3 to 6 mol% Y_2O_3 were t- and c-phases. Fig. 5 is an example of cubic/tetragonal two-phase structure in alloy 3. The diffraction pattern from matrix is indexed by an f c c lattice with a fluorite structure, but forbidden reflections appear from the second phase as in Fig. 5. The lenticular-shaped second phase was, therefore, recognized to be t-phase, which was embedded in cubic matrix [13]. The size of t-phase in Fig. 5 is much larger than that produced by ageing of PSZ [5, 13]. The t-phase in present alloys was mostly such a large one as in Fig. 5, but fine t-phase was also observed

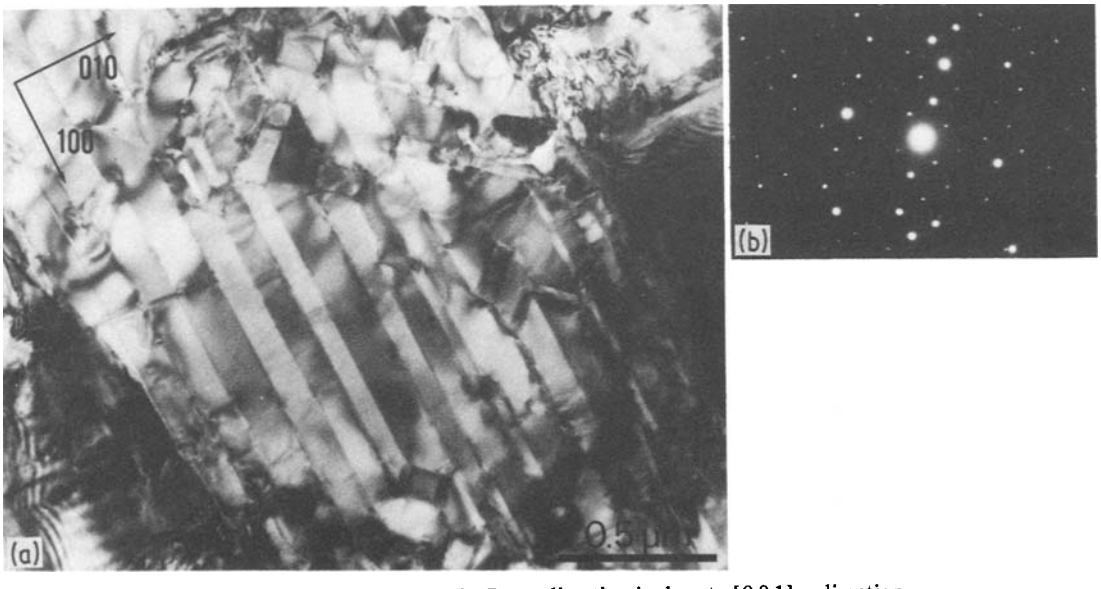

Figure 4 Twinned monoclinic phase in pure zirconia. Beam direction is close to $[0\,0\,1]_m$ direction.

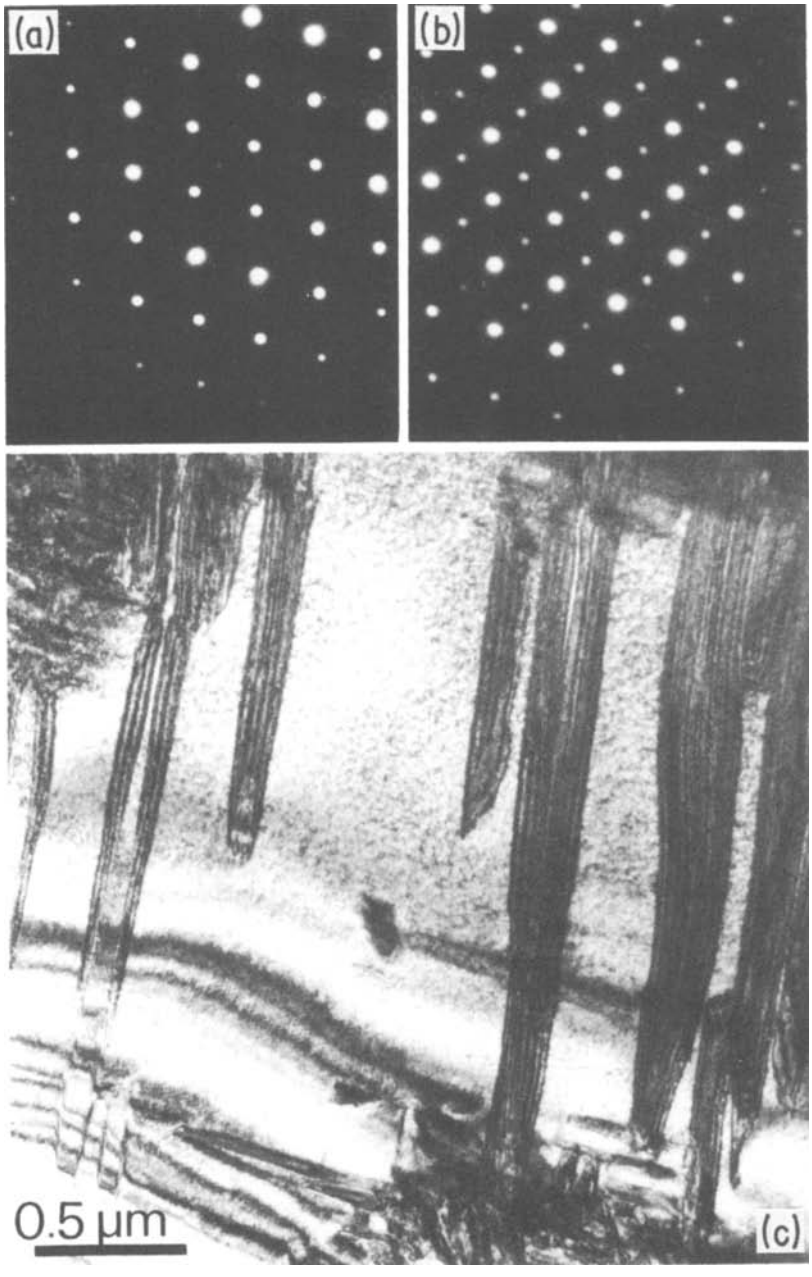

Figure 5 Lenticular t-phase embedded in cubic matrix in alloy 3. The diffraction pattern from matrix (a) is indexed by fluorite structure, but forbidden reflections in f c c lattice appear in the pattern from lenticular phase (b).

which was usually generated at the edge of large t-phase (Fig. 6).

Together with t- and c-phases, a phase with a characteristic "herring-bone" appearance was found in alloys 2 and 3. The microstructure of the phase shown in Fig. 7 is clearly different from the cubic/tetragonal two-phase structure. The phase with a herring-bone structure was regarded to be a metastable rhombohedral phase, because the diffraction pattern from the phase is distorted from that of fluorite lattice [25], and the microstructure is similar to rhombohedral β-phase in ZrO_2–Sc_2O_3 [26, 27]. The r-phase in PSZ was first found on the abraded surface [28]. The present result shows that the r-phase appears in ZrO_2–Y_2O_3 alloys with yttria content between 2 and 3 mol% as well as

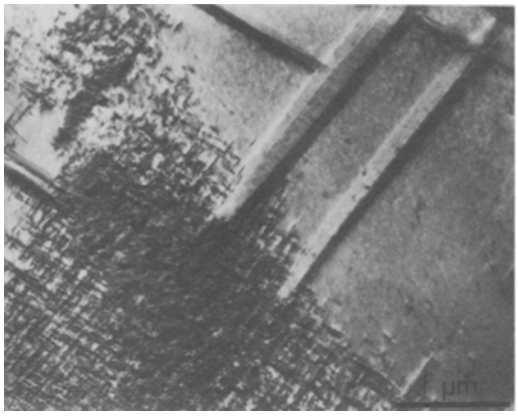

Figure 6 Fine t-phase found in alloy 3, which is usually formed at the edge of large t-phase.

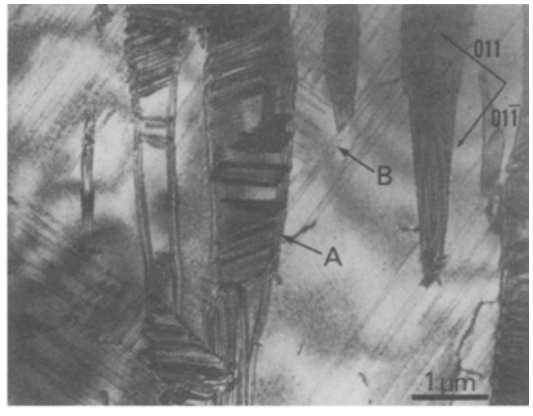

Figure 8 Two-phase structure of alloy 6. Lenticular (A) and thin-plate (B) t-phases are formed in the alloy. Note that the lenticular t-phase is twinned. Beam direction is near the $[1\,0\,0]_c$ direction in cubic phase, and the habit plane is close to $\{1\,1\,0\}_c$ plane.

abraded surfaces. The r-phase was found in alloys 2 and 3 by electron microscopy, but was not detected by X-ray diffraction on crushed powders. The result will be discussed in a later section. The r-phase disappeared in alloys with more than 4 mol % Y_2O_3, and only cubic/tetragonal two-phase structure was observed in alloys 4, 5 and 6. The two-phase structure was mostly similar to that in Fig. 5, but t-phase with thin-plate morphology was sometimes found in alloy 6 together with a lenticular-shaped one (Fig. 8). Thin-plate t-phase has a straight habit plane, which is close to $\{1\,1\,0\}_c$ plane. Twin-like faults are seen in lenticular-shaped t-phase in Fig. 8.

The structure of alloy 8 was composed of a single c-phase in which dislocations are sometimes found (Fig. 9). They were probably induced during cooling from the melting temperature.

4. Discussion

The present study on yttria-stabilized zirconia with a uniform composition has revealed that the microstructure sensitively changes with composition. The change in microstructure is closely related to the phase stability of ZrO_2–Y_2O_3 alloys. The phase appearing at room temperature varies with yttria content as shown in Fig. 1. The result shown in Fig. 1 agrees fairly well with the previous one obtained by X-ray diffraction analysis [14]. However, several new pieces of evidence were obtained on the microstructure of ZrO_2–Y_2O_3 alloys in this work. First of all, the phase with a herring-bone structure was found in alloys 2 and 3, which is likely to be a metastable

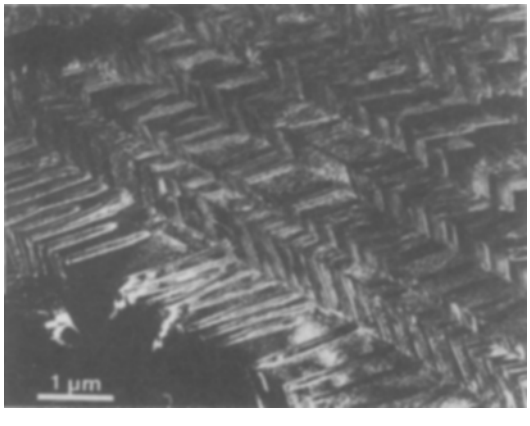

Figure 7 Herring-bone structure formed in alloy 3.

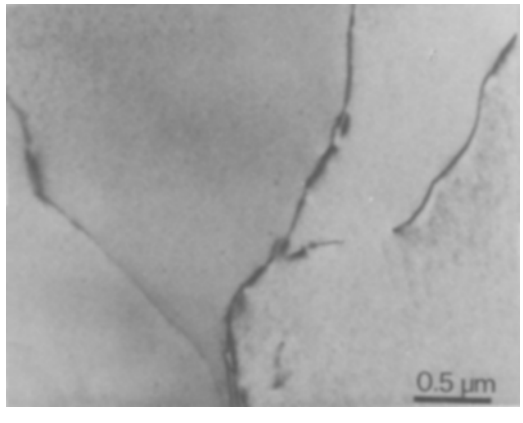

Figure 9 Structure of alloy 8, which is composed of single cubic phase. Dislocations are sometimes seen in the cubic phase.

r-phase. Secondly, the size and morphology of the t-phase are not necessarily the same as those reported previously [5, 13]. In the following section, the origin of the microstructure of the present alloys is discussed and then the role of microstructure on hardness and toughness is surveyed.

4.1. Rhombohedral phase appeared in PSZ

The phase with a herring-bone appearance was regarded to be a metastable r-phase in the ZrO_2–Y_2O_3 alloys. Microanalysis by scanning transmission electron microscopy revealed that the r-phase has a uniform yttrium content as expected from the average composition of each alloy. The result means that the diffusion of yttrium is very limited during cooling from melting temperature in the present alloys because of a fairly high cooling rate as mentioned previously. A short-range diffusion of yttrium or oxygen might occur, but extensive diffusion of yttrium did not occur during cooling. It is, therefore, likely that the r-phase is formed by martensitic (or bainitic) transformation during cooling.

The r-phase has not been detected in bulk PSZ prepared by a conventional process. The PSZ fabricated by sintering or hot-pressing is usually fired at cubic/tetragonal two-phase region and then cooled slowly to avoid introducing microcracks due to thermal shock. Firing at the two-phase region causes a development of local compositional fluctuation by cubic/tetragonal phase separation, and the subsequent slow cooling will also induce an additional diffusional transformation. Thus, the fabrication process of commercial PSZ is unlikely to generate r-phase during cooling, if the r-phase is formed by a martensitic transformation in the alloys with a particular composition. The appearance of r-phase by mechanical polishing also supports that the r-phase is produced by a martensitic transformation, which is often induced by mechanical treatments [29].

It is also noted that the r-phase was not detected by X-ray diffraction analysis of the crushed powders. For example, all the peaks from the crushed powders of alloy 3 were well-explained by t- or c-phase. The fact seems to indicate that the r-phase is transformed to a t-phase during the crush. It has been proposed that the r-phase in PSZ only exists in surface layer under stressed condition, because the powders removed from abraded surface gave rise to peaks from c-, t- and m-phases, and not from r-phase [28]. The stress is probably one of the factors to generate the r-phase. However, the present result suggests that the appearance of r-phase is not only affected by stress or mechanical treatments, but also affected by composition of PSZ, i.e. the stability of r-phase is dependent on composition. More details on the stability and also crystallographic features of the r-phase will be reported in a separate paper.

4.2. Size and morphology of t-phase

The lenticular-shaped t-phase in the present alloys generally has a length 1 to 5 μm and a width 0.1 to 0.3 μm, which are much larger than the t-phase formed by precipitation in cubic matrix during ageing [5, 13]. Fig. 10 shows the photograph of cubic/tetragonal two-phase structure together with the data of energy dispersive X-ray analysis. As known from the figure, the yttrium content is almost the same in t-phase and cubic matrix within an accuracy of the analysis. The fact means that the t-phase is not formed by a diffusional process

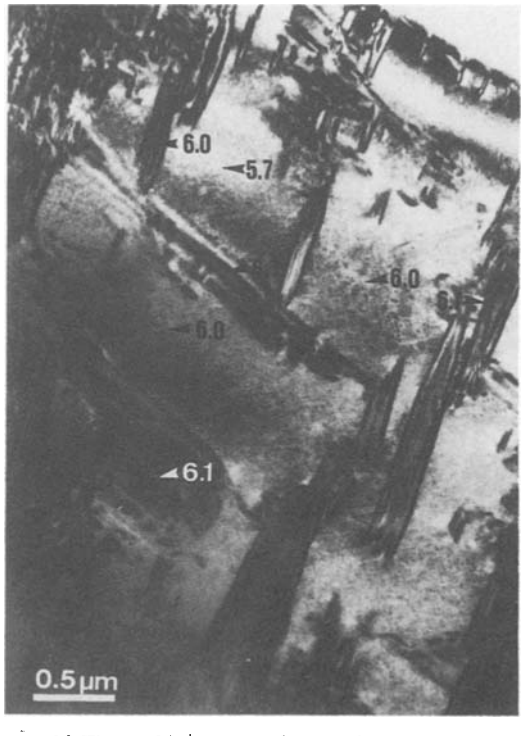

Figure 10 The cubic/tetragonal two-phase structure of alloy 6. Lenticular t-phase is embedded in cubic matrix. The figures in the photograph show the yttria content in local area, which was estimated by energy dispersive X-ray analysis. Note that the yttria content in t-phase is not different from cubic matrix within an accuracy of the analysis.

such as precipitation, but is rather likely to be formed by martensitic (or bainitic) reaction as well as r-phase. The t-phase is not necessarily internally-twinned or dislocated as often found in martensite [29]. The strain condition in the c → t transformation may satisfy the invariant plane strain condition [30].

Another interesting point is that the thin-plate t-phase sometimes observed in alloy 6 together with lenticular-shaped one (Fig. 8). The morphological change from lenticular to thin-plate martensite has been found in a number of iron alloys [31–39]. The generation of thin-plate martensite in iron alloys is associated with the fact that the transformation products are easily deformed by twinning rather than shear [40–42]. The thin-plate t-phase appears with internally-twinned lenticular t-phase in Fig. 8. The figure seems to show that twinning is easier in alloy 6 than in the other alloys with lower yttria content, because the internally-twinned t-phase was not seen in alloys with less than 5 mol% Y_2O_3. In agreement with iron alloys, thin-plate t-phase is found in alloys, in which twinning is possible to occur in t-phase.

4.3. Change in hardness and toughness with yttria content

Fig. 1 shows that the hardness and toughness of ZrO_2–Y_2O_3 alloys are markedly dependent on composition of alloys. The room-temperature phases in the alloys change sensitively with composition, which results in composition dependence of hardness and toughness.

The hardness of alloys increases at first rapidly and then slowly with increasing yttria content. The initial rapid increase in hardness occurs in the range of yttria content up to 3 mol%, which coincides with a marked decrease in m-phase with yttria content of alloys (Fig. 3). The m-phase is probably softer than t- or c-phase and the hardness would be sensitive to the amount of m-phase. On the other hand, the toughness change with composition is different from hardness change. The toughness of alloy 2 is much superior to other alloys. As mentioned previously, m-phase was rarely seen in thin foils prepared from as-cast button of alloy 2, but the volume fraction of m-phase in heavily-crushed powders of the alloy was about 0.5 as shown in Fig. 3. It seems that t-phase in alloy 2 was transformed to m-phase during the crush. The result means that the t → m transformation easily occurs during fracture in the alloy. The improved toughness of alloy 2 is probably caused by transformation toughening as proposed by previous workers [6–11].

A metastable r-phase was found in alloys 2 and 3, which have better toughness than the other alloys. The presence of r-phase may also be effective for improving the toughness of PSZ. However, the role of the r-phase on the toughness of PSZ is not clear, because the available information on r-phase is very limited at present.

Another point found in this work is that the alloys 4, 5 and 6 with cubic/tetragonal two-phase structure are lacking in toughness. The result means that the presence of t-phase in the cubic matrix is not necessarily effective for toughening PSZ. The yttria content of the t-phase is as high as average content of alloys. The t-phase with high yttria content was stably present in heavily crushed powders for X-ray diffraction analysis. The stable t-phase will not be transformed to m-phase during fracture and is ineffective for improving the toughness of PSZ.

5. Conclusions

ZrO_2–Y_2O_3 alloys with yttria content up to 8·7 mol% were prepared by arc-melting. The microstructural change with yttria content was examined mainly by electron microscopy, and the relationship between microstructure and mechanical properties was also surveyed. The microstructure developed in the alloys was considered to be formed by martensitic (or bainitic) transformation during fairly rapid cooling from melting temperature. Pure zirconia with single m-phase is inferior in hardness and toughness, but an addition of yttria causes an improvement of both properties. The hardness increase due to yttria addition up to 3 mol% Y_2O_3 is rapid, while further addition results in a very slight change in hardness. The rapid increase in hardness is associated with decrease in the amount of m-phase. The toughness of alloy 2 is much superior to other alloys. The t-phase with relatively low yttria content in the alloy is transformed to m-phase during fracture, and gives rise to improved toughness of PSZ. The toughness is inferior in alloys with more than 4 mol% Y_2O_3, which have either cubic/tetragonal two-phase structure or single cubic phase structure. The t-phase in the alloys is stable due to high yttria content and does not contribute to improve the toughness of PSZ.

Acknowledgements

Authors wish to express their sincere thanks to Mr K. Shibatomi JEOL Co Ltd for making an energy dispersive X-ray analysis by JEM 200CX electron microscope.

References

1. R. C. GARVIE, R. R. HUGAN and R. T. PASCOE, *Nature* **258** (1975) 703.
2. *Idem*, *Mater. Sci. Res.* **11** (1978) 263.
3. R. C. GARVIE, R. H. J. HANNINK and C. URBANI, Proceedings of the 4th International Meeting on Modern Ceramics Technologies, Saint-Vincent, Italy, May 1979 (Elsevier, Amsterdam, Oxford, New York, 1979) p. 692.
4. T. K. GUPTA, F. F. LANGE and J. H. BECHTOLD, *J. Mater. Sci.* **13** (1978) 1464.
5. D. L. PORTER and A. H. HEUER, *J. Amer. Ceram. Soc.* **62** (1979) 298.
6. D. L. PORTER, A. G. EVANS and A. H. HEUER, *Acta Metall.* **27** (1979) 1649.
7. N. CLAUSSEN and G. PETZOW, Proceedings of the 4th International Meeting on Modern Ceramic Technologies, Saint-Vincent, Italy, May 1979 (Elsevier, Amsterdam, Oxford, New York, 1979) p. 680.
8. A. G. EVANS and A. H. HEUER, *J. Amer. Ceram. Soc.* **63** (1980) 241.
9. N. CLAUSSEN and M. R. RUHLE, "Advances in Ceramics", Vol. 3, Science and Technology of Zirconia (The American Ceramic Society, Columbus, Ohio, 1981) p. 137.
10. C. A. ANDERSSON and T. K. GUPTA, *ibid.* p. 184.
11. F. F. LANGE and T. K. GUPTA, *ibid.* p. 217.
12. M. RAMADASS, S. C. MOHAN, S. R. REDDY, R. SRINIVASAN and S. G. SANDANI, *Mater. Sci. Eng.* **60** (1983) 65.
13. T. SAKUMA, Y. YOSHIZAWA and H. SUTO, *J. Mater. Sci.* **20** (1985) 1085.
14. H. G. SCOTT, *ibid.* **10** (1975) 1527.
15. K. NIIHARA, R. MORENA and D. P. H. HASSELMAN, *J. Mater. Sci. Lett.* **1** (1982) 113.
16. B. R. LAWN and D. B. MARSHALL, "Fracture Mechanics of Ceramics", Vol. 3, edited by R. C. Bradt, D. P. H. Hasselman and F. F. Lange (Plenum Press, New York, 1978) p. 205.
17. A. G. EVANS, *ibid.* p. 301.
18. P. CHANTIKUL, G. R. ANTIS, B. R. LAWN and D. B. MARSHALL, *J. Amer. Ceram. Soc.* **64** (1981) 539.
19. B. MUSSLER, M. V. SWAIN and N. CLAUSSEN, *ibid.* **65** (1982) 566.
20. M. V. SWAIN and N. CLAUSSEN, *ibid.* **66** (1983) c-28.
21. R. P. INGEL, R. W. RICE and D. LEWIS, *ibid.* **65** (1982) c-108.
22. E. C. SUBBARAO, H. S. MAITI and K. K. SRIVASTAVA, *Phys. Status Solidi (a)* **21** (1974) 9.
23. J. E. BAILEY, *Proc. Roy. Soc.* **279A** (1964) 395.
24. E. BISCHOFF and M. RUHLE, *J. Amer. Ceram. Soc.* **66** (1983) 123.
25. T. SAKUMA, Y. YOSHIZAWA and H. SUTO, *J. Mater. Sci. Lett.* **4** (1985) 29.
26. R. RUH, H. J. GARRETT, R. F. DAMAGALA and V. A. PATEL, *J. Amer. Ceram. Soc.* **60** (1977) 399.
27. F. K. MOGHADAM, T. YAMASHITA, R. SINCLAIR and D. A. STEVENSON, *ibid.* **66** (1983) 213.
28. H. HASEGAWA, *J. Mater. Sci. Lett.* **2** (1983) 91.
29. J. W. CHRISTIAN, "The Theory of Transformation in Metals and Alloys" (Pergamon Press, Oxford, 1965).
30. B. A. BILBY and J. W. CHRISTIAN, *Inst. Met. Monograph* No. 18 (1955) p. 121.
31. T. MAKI, S. SHIMOOKA, S. FUJIWARA and I. TAMURA, *Trans. Jpn. Inst. Metals* **16** (1975) 35.
32. M. UMEMOTO, E. YOHSITAKE and I. TAMURA, *J. Mater. Sci.* **18** (1983) 2893.
33. I. TAMURA, Proceedings of the 1st International Symposium on New Aspects of Martensitic Transformation, Supplement to *Trans. Jpn. Inst. Metals* **17** (1976) 59.
34. M. WATANABE and C. M. WAYMAN, *Met. Trans.* **2** (1971) 2221, 2229.
35. E. HORNBOGEN and W. A. MEYER, *Z. Metallkde.* **58** (1967) 372.
36. T. MAKI, K. KOBAYASHI and I. TAMURA, Proceedings of the 7th International Conference on Martensitic Transformations (ICOMAT-82) Leuvens, Belgium (1982) C4-541.
37. D. P. DUNNE and C. M. WAYMAN, *Met. Trans.* **5** (1974) 2047.
38. S. KAJIWARA and W. S. OWEN, *ibid.* **5** (1973) 137, 147.
39. M. UMEMOTO and C. M. WAYMAN, *Acta Metall.* **26** (1978) 1529.
40. D. P. DUNNE, *Scripta Metall.* **11** (1977) 1017.
41. S. KAJIWARA and W. S. OWEN, *ibid.* **11** (1977) 137.
42. M. S. WECHSLER, D. S. LIEVERMAN and T. A. READ, *Trans. AIME* **197** (1953) 1503.

Received 10 July
and accepted 31 July 1984